Elliptical Slot Circular Patch Antenna Array with Dual Band Behaviour for Future 5G Mobile Communication Networks

**Muhammad I. Khattak[1, *], Amir Sohail[1], Ubaid Khan[1],
Zaka Ullah[1], and Gunawan Witjaksono[2]**

Abstract—This paper presents a dual band circular microstrip patch antenna with an elliptical slot for future 5G mobile communication networks. The antenna has resonating frequencies of 28 GHz and 45 GHz, with bandwidths of 1.3 GHz and 1 GHz, respectively. Efficiency of the antenna is 85.6% at 28 GHz and 95.3% at 45 GHz. The return loss at 28 GHz is -40 dB, with maximum gain of 7.6 dB while at 45 GHz return loss is -14 dB with maximum gain of 7.21 dB. The antenna is designed on a Rogers RT5880 (lossy) substrate with dielectric constant of 2.2 and loss tangent ($\tan \delta$) of 0.0013. The antenna has a compact size of $6 \times 6 \times 0.578$ mm^3. Array configuration is used to achieve 12 dB gain, required for mobile communication. The proposed array has resonance frequencies of 28 GHz, 34 GHz and 45 GHz with maximum gain of 13.5 dB and radiation efficiency of 98.75%. Centre series fed technique is used for the excitation of array. SAR value of array antenna obtained at 28 GHz is 1.19 W/kg, at 34 GHz is 1.16 W/kg, and at 45 GHz is 1.2 W/kg. CST Microwave Studio, a 3D simulating tool, is used for the antenna design and calculation of the antenna parameters along with the SAR analysis.

1. INTRODUCTION

Mobile wireless technology has been assessed from 0G to 4G, bringing the revolution in mobile communications [1, 2]. Each generation is an old, improved version [2]. 4G technology has many applications, such as remote host monitoring, video call data flow and machine type communication [2]. 4G has some advantages but is unable to solve the problems of poor quality, poor coverage, loss of connections, high energy consumption, bad interconnectivity and overcrowded channels [3, 4]. Due to the rapid growth of communication system connected devices, current 4G technology will not meet the recent demand [5]. Therefore, the mobile communication system must be upgraded to the next generation (5G) in order to meet the future demand of high data rates [6]. Research is underway for 5G mobile communications and is expected to be commercialized early in the 21st century [4, 7].

With rapid increase in user equipment, the bandwidth requirement is also increased to enable the flow of large amount of data [8]. The exponential increase is expected in a number of devices such as HD TVs, laptops, smart phones, home appliances, video surveillance systems, sensors, wearable devices, cameras and robots in near future. 5G technology promises the required data rate and bandwidth for such applications [9] such that 5G mobile communication is expected to assist large number of real time applications, tactile internet [10] and services with different levels of quality (QoS) (like, bandwidth, jitter, packet delay, latency and packet loss) and quality of experience (like network providers and users). The high-speed data transfer, zero latency and ubiquitous connectivity are the main characteristics of 5G technology. 5G technology will interconnect every electronic and digital appliance/services like temperature maintenance, printers, air conditioners, refrigerators, LED's door locks, microwave oven,

etc. and will enable remote control of such appliances [11]. 5G technology is considered as a real wireless world with no limitations, which will develop worldwide wireless web and dynamic ad-hoc wireless network [12]. It also offers high resolution and bidirectional large bandwidths in giga bits to make advance billing interface more attractive and effective with the special provision of multiple paths for data transfer [13].

5G technology was introduced in a new era of digital mobile communications systems, which introduces the Internet of Things (IOTs) into the network of devices (D2Ds) [14, 15] with wider bandwidth [16], lower battery consumption, higher data rates and better coverage [14, 17], and will solve various challenges such as latency, security, reliability, availability and equipment costs [18]. Spectrum allocation is one of the main concerns of 5G communications. The fifth generation of mobile communications is being studied in the millimeter wave band [14, 19, 20]. Some of the expected bands recommended for 5G mobile communications are: 27.5–29.5 GHz, 33.4–36 GHz, 37–40.5 GHz, 42–45 GHz, 47–50.2 GHz, 50.4–52.6 GHz and 59.3–71 GHz [6]. However, for cellular communications, the 28 GHz and 38 GHz bands are advantageous [6, 21], but operating at higher frequency bands will bring complexity in the antenna design of mobile communication system [2].

Microstrip patch antennas are of great interest due to higher data rate and directional radiation for wireless applications. Heinrich Hertz in 1886 demonstrated a patch antenna for the first time, and in 1901, Guglielmo Marconi gave its practical application. The first practical antenna was designed in early 1970s by Howell and Muson. For practical applications, bandwidth and size of the antenna are the main concern for antenna designers. Microstrip patch antennas have numerous advantages like low cost, small size, high efficiency, easy manufacturing and fabrication [22–25] and are mechanically robust when being mounted on a rigid surface [26]. Dual and triple band operational frequencies can be easily achieved with minimal efforts along with various polarizations of E-fields by using different feeding methods and shapes of radiation patches [27]. Microstrip antennas are widely used in Global Positioning System (GPS), wireless local area network, mobile communication system, and microwave sensors [28, 29]. Despite of these attractive advantages, microstrip antennas also have some limitations which include narrow bandwidth [30] and low gain. Research shows that bandwidth can be improved using different methods such as using slotted patch, thick substrates [31], substrate of low effective permittivity, incorporating multiple resonances, and optimizing impedance matching [32]. Array configuration is implemented to improve the gain limitations [33].

Particularly for the fifth generation mobile communications, recently some researchers have put forward various patch antenna designs. A compact patch antenna for 5G mobile communications has been presented by the authors of [3] with resonant frequencies at 10.15 GHz and 28 GHz and maximum gains of 5.51 dB at 10.15 GHz and 8.03 dB at 28 GHz. The antenna was designed using a Rogers-5880 substrate with thickness of 0.787 mm and total area of $21 \times 21 \, mm^2$. The authors of [34] presented a PIFA antenna for 5G application with operating frequencies of 28 GHz and 38 GHz consisting of shorted patch with a U-shape slot etched in the radiating patch. The maximum gain obtained at 28 GHz is 3.75 dB and 5.06 dB at 38 GHz. An FR-406 substrate is used to isolate ground and the patch. Ali et al. proposed a small antenna, excited with coplanar waveguide (CPW) feed, attaining a maximum gain of 6.6 dB at 28 GHz, while a Roger RT5880 substrate is used with the size of $5 \times 5 \, mm^2$ and height of 0.254 mm [35]. In [36], the authors have introduced an antenna array for 5G cellular networks and MIMO applications. This array network helped in achieving a maximum gain of 6.6 dB at 28 GHz. The authors of [37] presented a 5G capable slotted microstrip patch antenna having a resonance frequency at 11 GHz with a compact size of $22 \times 19 \, mm^2$. The antenna has a directivity of 6.348 dB and maximum gain of 6.3 dB. In [38], the authors introduced a compact antenna using a microwave dielectric ceramics substrate for 5G applications with small size dimensioning as $14 \times 14 \, mm^2$. The maximum gain for the design is 5.4 dB with 93% radiation efficiency. The authors of [39] presented a T and L-shaped slotted microstrip patch antenna for future 5G mobile and wireless communication, using FR4 epoxy material as the substrate with dimensions of $10 \times 10 \times 1.6 \, mm^3$. The operating frequency of the antenna here is 28 GHz with the highest gain of 5.57 dB for the said resonant frequency.

The design complications such as complexity and larger size along with low radiation efficiency, low gain are some of the main concerns associated with the cited research. Table 1 summarizes the details of the cited work. The aim of this research is, therefore, to overcome the low performance and design complexity of the microstrip patch antenna for 5G mobile communication networks. An easy to

Table 1. Comparison of size, gain and efficiency of different antennas.

Reference paper	Antenna size (mm^2)	Operating frequency (GHz)	Gain (dB)	Efficiency (%)
[3]	21 × 21	10, 28	7.5	62
[34]	3 × 7	28, 38	3.7	69
[35]	5 × 5	28	6.6	73
[36]	120 × 40	28	6.6	77
[37]	22 × 19	11	6.3	-
[38]	14 × 14	28	5.4	93
[39]	10 × 10	28	5.57	-
This work	6 × 6	28, 45	7.6, 7.21	85.6, 95.3

fabricate microstrip patch antenna is proposed here, having an elliptical slotted circular radiating patch over a Roger RT-5880 substrate, due to its low dielectric constant and low loss dispersion, which is considered as a suitable material for ultrahigh frequency (UHF). The required 12 dB gain and radiation pattern for mobile communication is achieved by using an array structure.

2. ANTENNA THEORY AND DESIGN

The first important step in designing an antenna was the selection of the substrate. The impedance matching and bandwidth of an antenna are highly influenced by the parameters of substrate like height, dielectric constant and tangent loss ($\tan \delta$). High copper losses may occur due to using a very thin substrate while a thicker substrate can degrade the performance of antenna due to surface waves. In the proposed antenna design, a Roger RT-5880 substrate is used whose dimensions and electrical properties are given in Table 2. To obtain the desired resonance frequency of 28 GHz, a circular patch of a particular radius (R_p) is used relating to Equation (1). The patch has an elliptical slot in order to improve the bandwidth of the antenna. The circular patch of the antenna is fed by using a 50 Ω microstrip line. Figure 1 shows different views of the unit cell, and its parameters are given in Table 3. The actual radius of the circular patch is calculated by the formula given by [40].

$$R_p = \frac{F}{\sqrt{1 + \frac{2h}{\pi \varepsilon F \left[\ln \left(\frac{F\pi}{2h} \right) + 1.7726 \right]}}} \tag{1}$$

where

$$F = \frac{8.791 \times 10^9}{f \sqrt{\varepsilon}} \tag{2}$$

R_p = the radius of the patch, h = the height of the substrate, f = the resonance frequency in hertz, ε = the effective dielectric constant of substrate.

Table 2. Dimensions and electrical properties of Rogers RT-5880.

Parameters	Values
Dielectric constant	2.2
Loss tangent	0.0013
Dimension	6 × 6 mm^2
Substrate height	0.508 mm

Table 3. Design dimensions of the proposed elliptical slotted patch antenna.

Parameters	Description	Value (mm)
Ls	Substrate Length	6
Ws	Substrate width	6
H	Substrate height	0.508
Rp	Patch radius	2
Dy	Diameter of slot on y-axis	2
Dx	Diameter of slot on x-axis	0.8
Mt	Patch Height	0.035
Wf	Feed line Width	0.38
Lg	Ground Length	6
Wg	Ground width	6

(a)   (b)   (c)
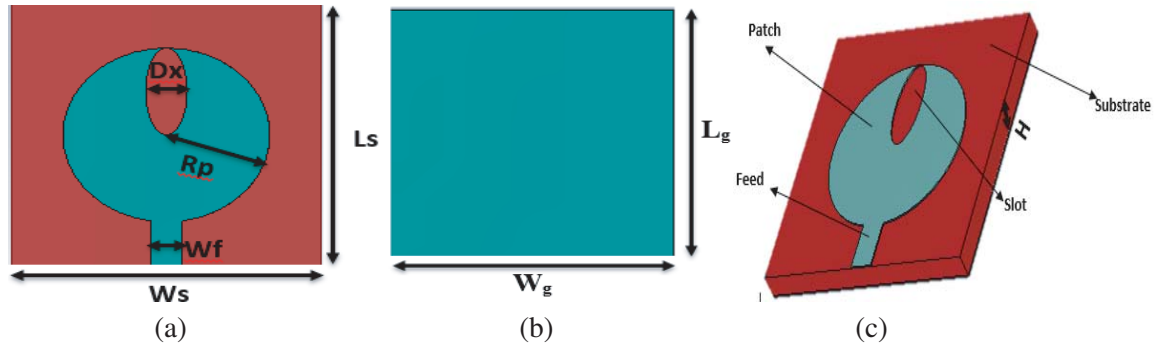
Figure 1. The proposed antenna design. (a) Front view, (b) back view and (c) perspective view.

2.1. Array Design

For the aim of achieving 12 dB gain for 5G Mobile communication applications, a series array of 1×4 elements is implemented. The array is fed at the centre, and the configuration is shown in Figure 2.
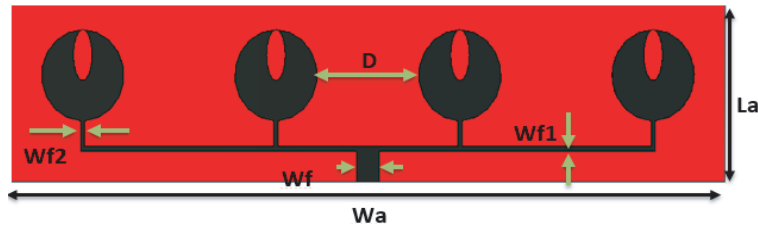
Figure 2. Front view of the proposed array with design dimension variables.

The array resonates at 28 GHz, 34 GHz and 45 GHz, respectively. The 34 GHz resonance frequency appears due to the introduction of a series feeding network on the substrate. Since the size of the unit cell is very small, the flux linkage of the radiating patch with conductors of the feeding network results in an extra resonance at 34 GHz. This phenomenon will be further clarified in the surface currents plot in Figure 8(b) in Results and Discussion Section. All elements of the array resonate at the same frequency and are designed for radiation in broadside direction. The array is split into two linear subarrays and fed

in the middle through quarter-wave transformer. The cross polarization level of the array is improved by this type of symmetric arrangement. It also prevents the beam pointing direction from varying with frequency. In this way, the cross polarization generated from two opposite sides of the array are cancelled out in broadside direction. Unit cells are kept 4.4 mm apart for the necessary prevention of the interference. The array is fed with center series fed technique. Dimensions of the array are given in the Table 4.

Table 4. Dimensions of the various design variables of the proposed array configuration.

Parameters	Description	Value (mm)
D	Distance b/w unit cells	4.4
Wa	Array width	31
La	Array length	7
Wf	Centre fed	1
$Wf_1 = Wf_2$	Series fed	0.19

3. RESULTS AND DISCUSSION

In this section the simulated and measured results of the proposed unit cell design of the antenna are discussed. In Part A and Part B VSWR and S_{11} (dB) commonly known as voltage standing wave ratio and return loss of the microstrip patch antenna as a unit cell and series fed 1×4 array configuration are presented. Parts C, D and E explain 2D plots of the radiation patterns, current distribution and 3D gain plots, respectively, of both microstrip patch antenna as a unit cell and 1×4 array configuration. Finally, the SAR analysis is performed for both the configurations.

3.1. VSWR

Impedance matching of the antenna and transmission line is a key factor in evaluating the antenna performance. VSWR parameter defines how well the impedance of antenna is matched with transmission line by taking the ratio of the reflected maximum and minimum voltage wave. A value of VSWR ≤ 2 is considered as the main requirement. The suggested antenna in this work has a VSWR value of 1.01 and 1.5 at resonating frequencies of 28 GHz and 45 GHz, respectively. Array of the proposed antenna has VSWR values of 1.15, 1.3 and 1.43 at 28 GHz, 34 GHz and 45 GHz, respectively. VSWRs of both unit cell and 1×4 array configurations are given in Table 5, and the respective graphs are shown in Figure 3.
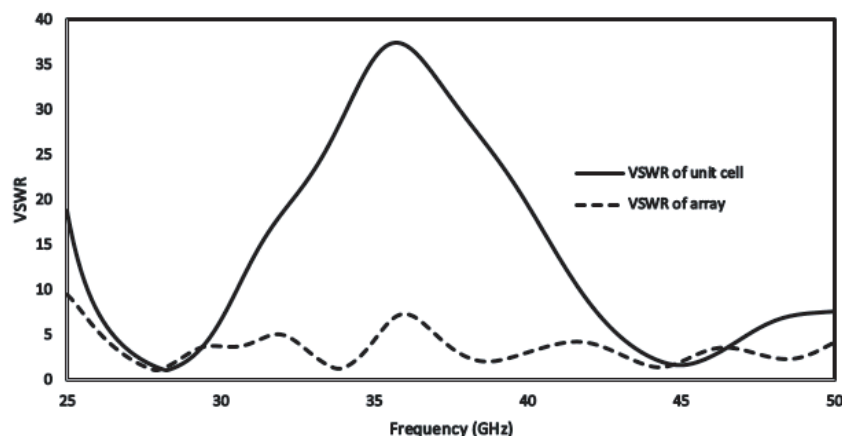

Figure 3. VSWR of the proposed antenna as (a) unit cell configuration and (b) array configuration.

Table 5. Voltage standing wave ratio (VSWR) values of unit cell and array configurations.

Antenna	Unit cell		Array		
Frequency (GHz)	28	45	28	34	45
VSWR	1.01	1.5	1.15	1.3	1.43

3.2. Return Loss

Return loss is the ratio of incident power to the reflected power of an antenna in decibels (dB). Return loss of an antenna is represented by S_{11} (dB). For an antenna to perform in effective way, S_{11} (dB) should be less than -10 dB. The proposed antenna has S_{11} (dB) of -40 dB and -14 dB at 28 GHz and 45 GHz, respectively, and array of the suggested antenna has return losses of -25.8 dB, -18 dB and -15 dB at 28 GHz, 34 GHz and 45 GHz, respectively, as shown in Table 6. The obtained results are optimized by changing the values of Dx and Dy. It can be clearly seen form Figures 4(a), (b) that for $Dx = 0.8$ mm and $Dy = 2$ mm better results are obtained. Moreover, changing these values can shift the resonance frequencies. Graphs of both the unit cell and 1×4 array configurations are given in Figure 4(c).

Table 6. Return loss (S_{11} (dB)) values of the proposed antenna as a unit cell and array configurations.

Antenna	Unit cell		Array		
Frequency (GHz)	28	45	28	34	45
Return loss (dB)	-40	-14	-25.8	-18	-15

The values of characteristic parameters of the proposed antenna as a unit cell and 1×4 array configurations in terms of gain, resonance frequency, directivity, bandwidth and efficiency are tabulated in Table 7.

Table 7. Characteristic parameters of the proposed antenna as a unit cell and array configuration.

Antenna	Resonance Frequency (GHz)	Bandwidth (GHz)	Efficiency (%)	Gain (dB)	Directivity (dBi)
Unit Cell	28	1.3	85.6	7.6	7.68
	45	1	95.3	7.21	7.26
Array	28	1.2	99.3	13.5	13.5
	34	0.92	94.7	11.2	11.5
	45	1.2	91.9	12.1	13.17

3.3. 2D-Polar Radiation Patterns of the Proposed Antenna

1) Unit Cell Configuration: The radiation patterns at various spot frequencies are presented in Figure 5. The solid line represents E-plane (XZ, $\emptyset = 0°$), and dashed line represents H-plane (YZ, $\emptyset = 90°$) radiation pattern. The radiation efficiencies at the spot frequencies of 28 GHz and 45 GHz are 85.6% and 95.3% respectively while directivities are 7.68 and 7.26 respectively for the targeted frequencies.

2) Array Configuration: The radiation patterns at various spot frequencies are presented in Figure 6. The solid line represents E-plane (XZ, $\emptyset = 0°$), and dashed line represents H-plane (YZ, $\emptyset = 90°$) radiation pattern. The radiation efficiencies at the spot frequencies of 28 GHz, 34 GHz and 45 GHz are 99.3%, 94.7% and 91.9% respectively while directivities are 13.5, 11.5 and 13.17 respectively for the targeted frequencies.
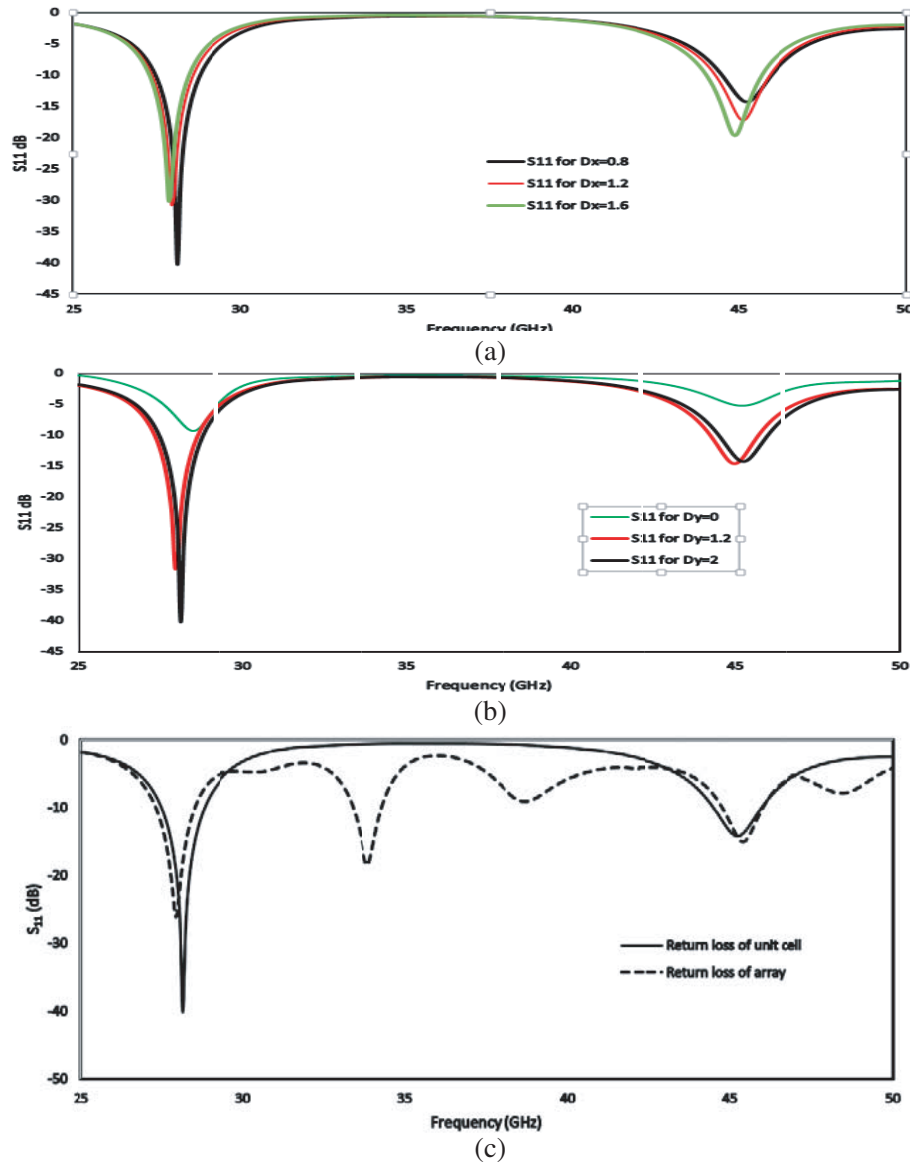
Figure 4. (a) Optimized S_{11} (dB) with respect to Dx, (b) optimized S_{11} (dB) with respect to Dy, (c) S_{11} (dB) of the unit cell and array configuration.

3.4. Surface Current Distribution

1) Unit Cell Configuration: Surface current distributions of microstrip antenna at target frequencies of 28 GHz and 45 GHz are given in Figure 7. At 28 GHz current distribution is maximum at the slot and circular edge, while at 45 GHz the current distribution is maximum at junction of the microstrip line and the radiating circular patch which causes the maximum radiation lobe to split to $\pm 30°$, and the same argument is valid for all such phenomena.

2) Array Configuration: Surface current distributions of array antenna at 28 GHz, 34 GHz and 45 GHz are shown in Figure 8.

3.5. 3D Gain Plots of the Proposed Antenna

1) Unit Cell Configuration: 3D gain plots for the unit cell configuration are shown in Figure 9 at the spot frequencies of 28 GHz and 45 GHz, respectively. It can be clearly observed from Figure 9 that
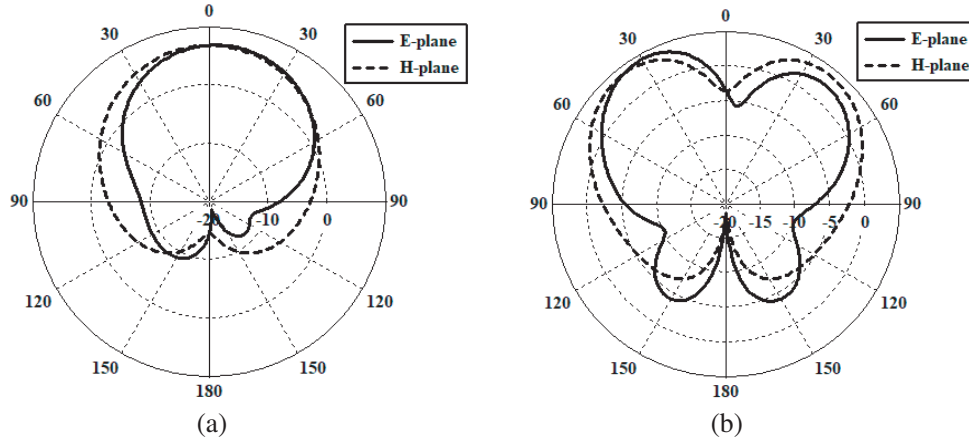
Figure 5. Polar plots of the unit cell at spot frequencies of (a) 28 GHz and (b) 45 GHz.
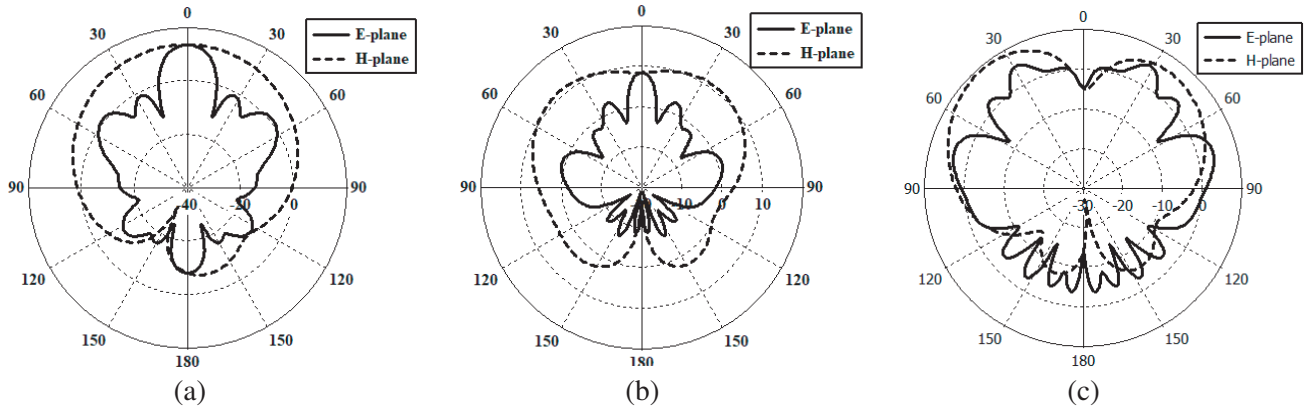

Figure 6. Polar plots of E and H plane of the array antenna at (a) 28 GHz, (b) 34 GHz and (c) 45 GHz.
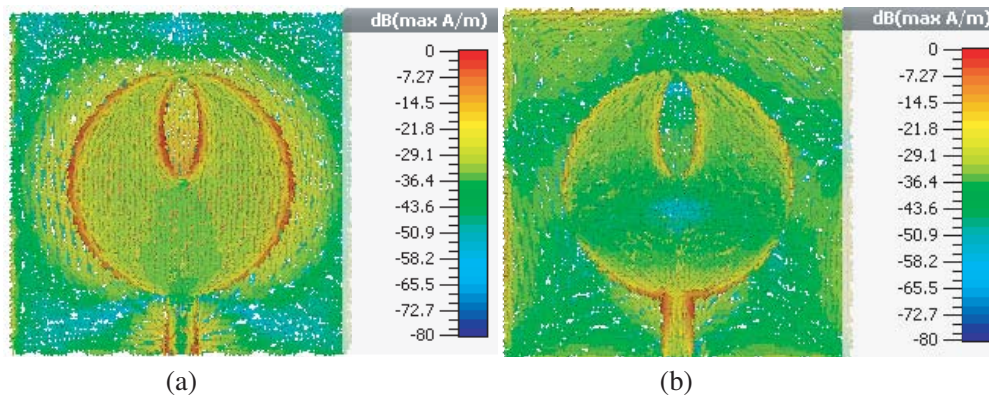

Figure 7. Surface current distribution of the unit cell configuration at spot frequencies of (a) 28 GHz and (b) 45 GHz.

the unit cell antenna exhibits monopole radiation pattern at both frequencies.

  2) Array Configuration: 3D gain plots for the array configuration are shown in Figure 10 at the spot frequencies of 28 GHz, 34 GHz and 45 GHz, respectively. It is observed from the figure below that with increase in gain the beamwidth becomes narrower.
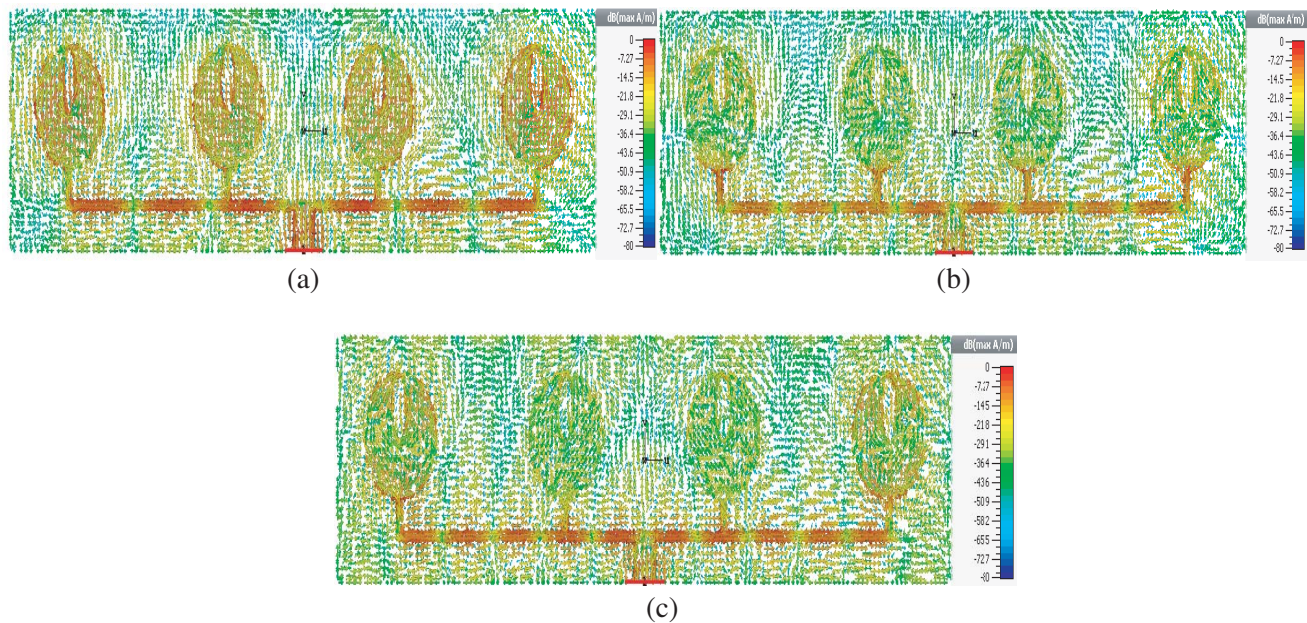
Figure 8. Surface current distribution of the array at spot frequencies of (a) 28 GHz, (b) 34 GHz and (c) 45 GHz.
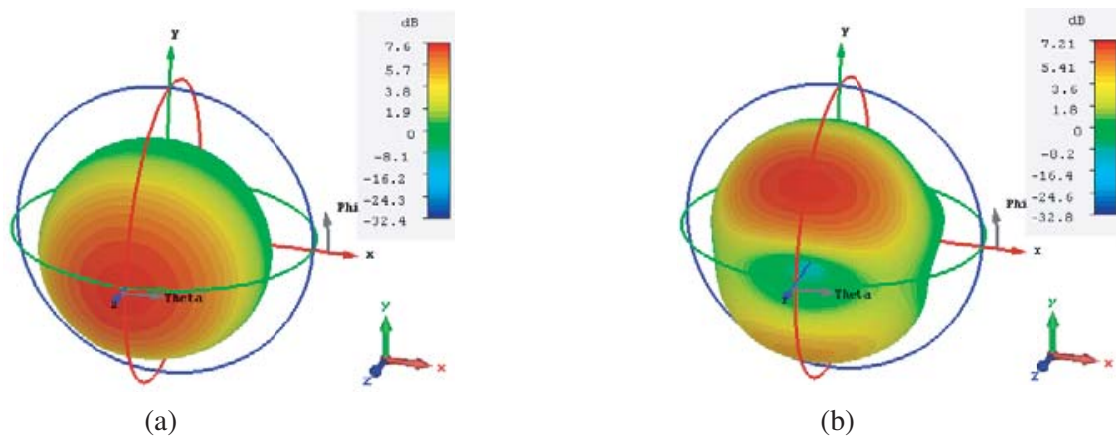

Figure 9. 3D Gain plots of the unit cell configuration at spot frequencies of (a) 28 GHz and (b) 45 GHz.

4. SAR ANALYSIS

Specific absorption rate (SAR) is a measure of the rate at which energy is absorbed by the human body from the RF electromagnetic fields. It has unit of watt per kilogram (W/Kg), and it is usually averaged over 1 g or 10 g sample of the tissue. SAR can be calculated as

$$\text{SAR} = \frac{\delta E^2}{2\rho} \tag{3}$$

where

    δ is the sample electrical conductivity

    E is the RMS electric field

    ρ is the sample density.

(a)   (b)   (c)
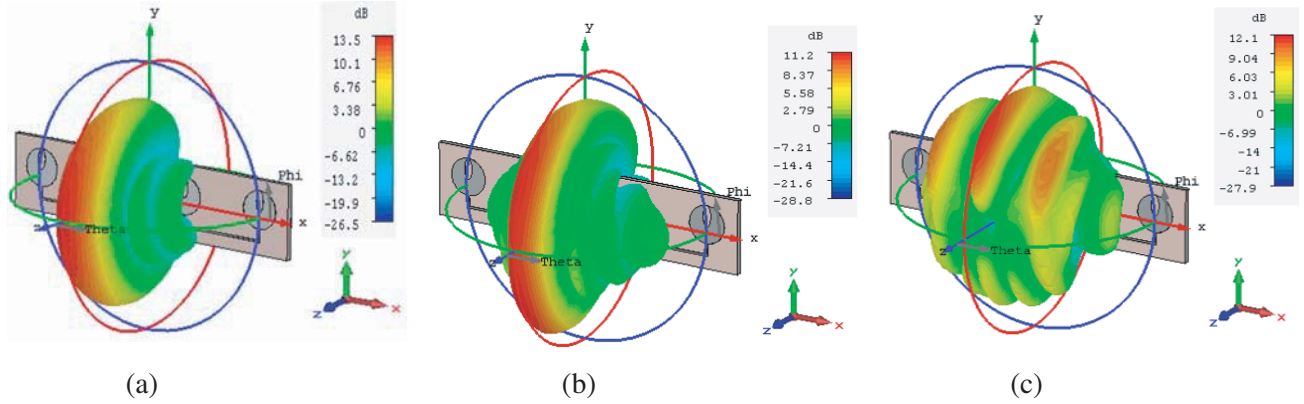
Figure 10. 3D gain plots of the array configuration at spot frequencies of (a) 28 GHz, (b) 34 GHz and (c) 45 GHz.

(a)   (b)
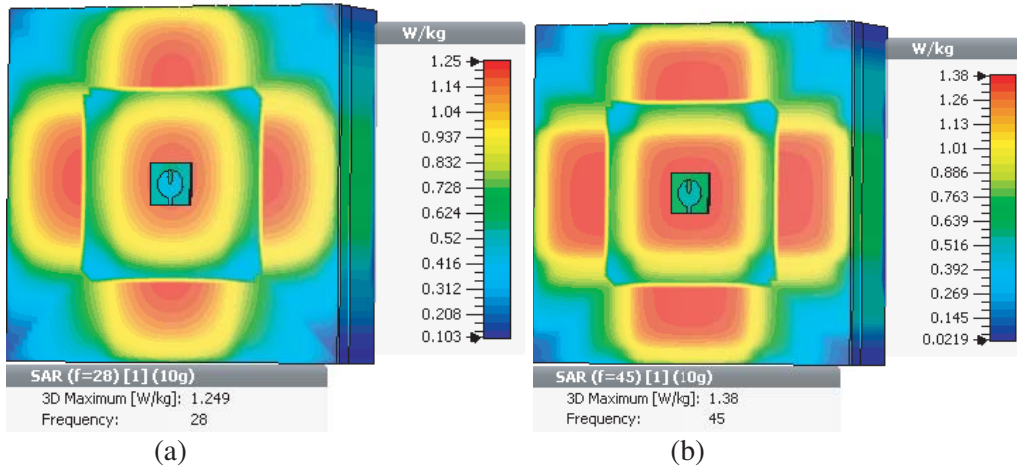
Figure 11. SAR analysis of the unit cell configuration at target frequencies of (a) 28 GHz and (b) 45 GHz.

The RF current in the antenna induces RF electric field, and the radiations produced by the induced RF field are absorbed by the body tissue and cause cell mutation. According to FFC and CENELEC SAR values must be a level at or less than 1.6 W/kg averaged over 1 g of tissue and 2 W/Kg taken over the volume containing mass of 10 g of the tissue. Figure 11 shows the view of SAR distribution on human body analysis at different frequencies for the unit cell while Figure 12 shows the SAR analysis of the 1×4 array configurations. To estimate radiation effects of the proposed antenna at different frequencies, 10 g mass test is used. In the case of unit cell, SAR value for 28 GHz is 1.25 W/kg and 1.38 W/kg at 45 GHz. For array configuration, SAR value at 28 GHz is 1.19 W/kg, at 34 GHz is 1.16 W/kg and at 45 GHz is 1.37 W/kg. SAR analysis is done on flat body model which consists of three layers that are skin, fats and muscle having length and width of $100 * 100\,\mathrm{mm}^2$. The thickness of skin is 3 mm; that of fat is 10 mm; and that of muscle is 20 mm, such layered body models are common in practice [41–43]. SAR values at all the resonating frequencies are less than SAR limit defined by telecom authorities. Values of SAR at all the operating frequencies for both unit cell and array antenna are shown in Table 8.

5. MEASURED RESULTS

The array antenna is fabricated using a Rogers RT5880 (lossy) substrate, with the height of 0.508 mm. The Anritsu 37369D 40 GHz VNA is used for measurement of S_{11} (dB) parameter. There is a reasonable
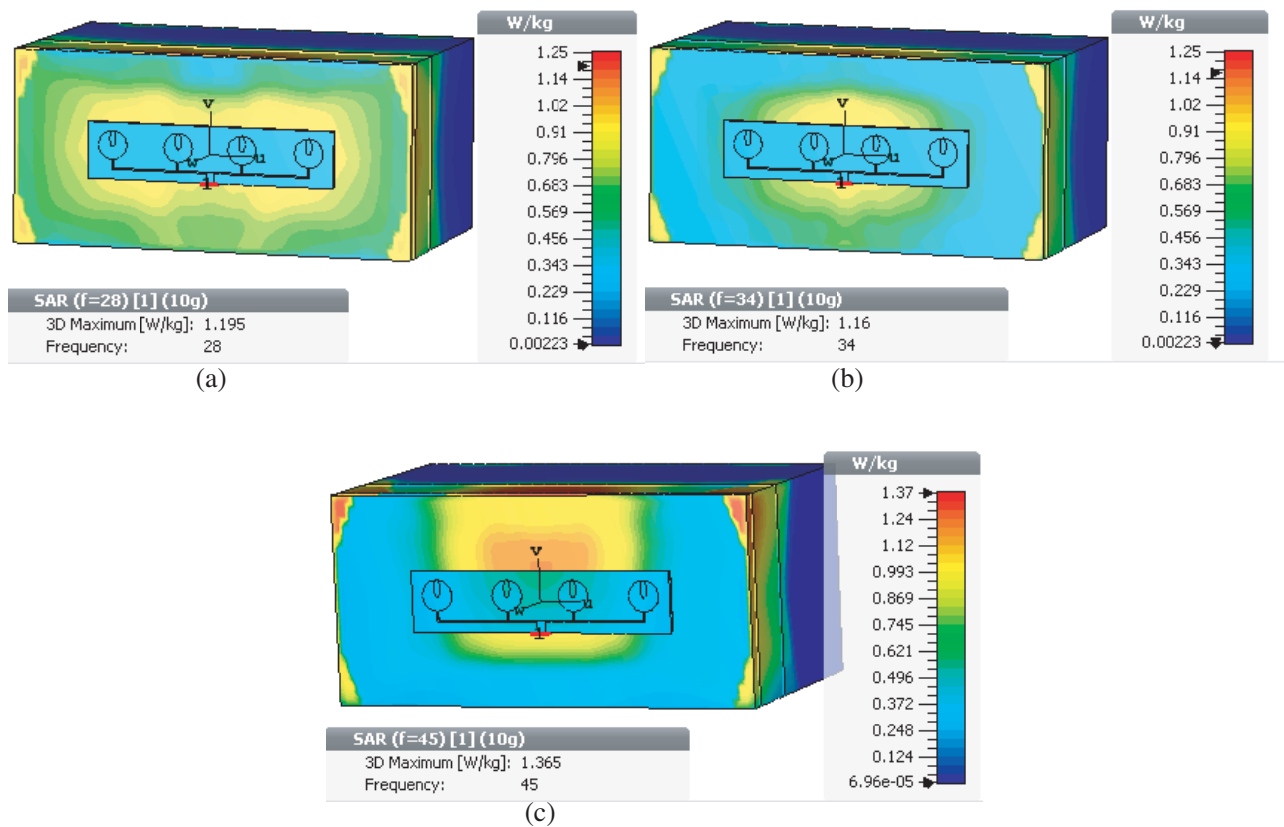
(a)   (b)

(c)

Figure 12. SAR analysis of the array configuration at target frequencies of (a) 28 GHz, (b) 34 GHz and (c) 45 GHz.
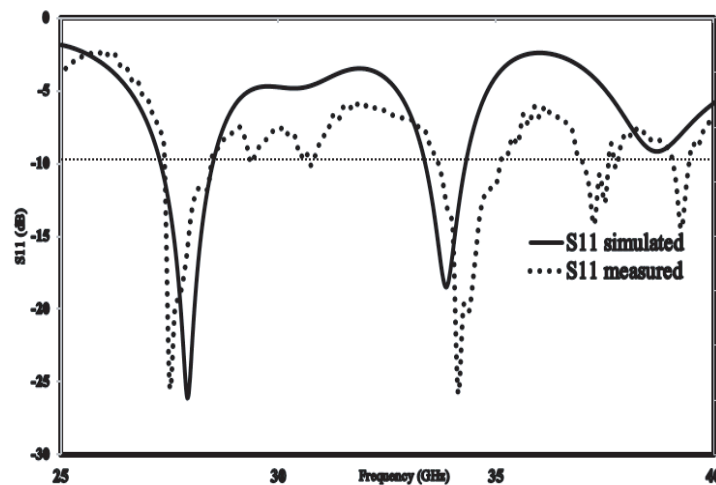

Figure 13. Measured and simulated return loss of the proposed array configuration for 5G mobile communications.

agreement between measured and simulated results as shown in Figure 13. Both the measured and simulated S_{11} (dB) graphs of the array antenna justify the required bands of operations for 5G applications. From the graph it is clear that the simulated S_{11} (dB) is less than -10 dB in the ranges of 27.4–28.6 GHz and 33.4–34.32 GHz, while measured S_{11} (dB) is less than -10 dB in the ranges of

Table 8. SAR values of the proposed antenna as a unit cell and array configurations for various spot frequencies.

Antenna	Unit cell		Array		
Frequency (GHz)	28	45	28	34	45
SAR value (W/Kg)	1.25	1.38	1.19	1.16	1.37

Figure 14. A photograph of the proposed array configuration for 5G mobile communications.

27.4–28.6 GHz and 33.75–35.125 GHz. A sample photograph of the fabricated array antenna with SMA 40 GHz connector is shown in Figure 14.

6. CONCLUSIONS

A novel dual band circular microstrip patch antenna with an elliptical slot is presented in this research for possible future 5G applications. The antenna is further configured to an array of 1×4 linear elements to make it suitable for 5G mobile communication systems. This simple design is achieved on a Rogers 5880 substrate which resonates at millimeter-wave frequencies of 28 GHz and 45 GHz as a unit cell and with an extra resonance at 34 GHz when be configured as an array. The maximum gain 7.6 dB is achieved at 28 GHz for unit cell and a gain of 7.21 dB at 45 GHz, and the gain is further enhanced to 13.5 dB at 28 GHz in array configuration to make the antenna system suitable for 5G mobile communications, with a gain of 11.2 dB at 34 GHz and 12.1 dB at 45 GHz. The directional properties of the radiation pattern are also simulated for the particular 5G application at the spot frequencies of 28 GHz, 34 GHz in the case of array and 45 GHz, and were found to be in good competition with designs already available in the literature. At the end one of the important aspects mandatory for hand-held/wearable applications, the SAR (Specific Absorption Rate), is also simulated, and in the case of unit cell, SAR value for 28 GHz is 1.25 W/kg and 1.38 W/kg at 45 GHz, and for array configuration, SAR value at 28 GHz is 1.19 W/kg, at 34 GHz is 1.16 W/kg and at 45 GHz is 1.37 W/kg. These values appear in accordance with the standards mentioned in FFC and CENELEC.

REFERENCES

1. Hakimi, S. and S. K. A. Rahim, "Millimeter-wave microstrip bent line grid array antenna for 5G mobile communication networks," *2014 Asia-Pacific Microwave Conference (APMC)*, 622–624, IEEE, November 2014.
2. Ojaroudiparchin, N., M. Shen, and G. F. Pedersen, "A 28 GHz FR-4 compatible phased array antenna for 5G mobile phone applications," *2015 International Symposium Antennas and Propagation (ISAP)*, 1–4, IEEE, November 2015.

3. Jandi, Y., F. Gharnati, and A. O. Said, "Design of a compact dual bands patch antenna for 5G applications," *2017 International Conference on Wireless Technologies, Embedded and Intelligent Systems (WITS)*, 1–4, IEEE, April 2017.

4. Reddy, N. K., A. Hazra, and V. Sukhadeve, "A compact elliptical microstrip patch antenna for future 5G mobile wireless communication," *IEEE Transactions on Engineering and Applied Sciences*, Vol. 1, No. 1, 1–4, 2017.

5. Loharia, N., S. B. Rana, and N. Kumar, "5G future communication: Requirements and challenges," *47 Mid-term Symposium on Modern Information and Communication Technologies for Digital India (MICTDI 2016)*, Chandigarh, India, 2016.

6. Kumar, A. and M. Gupta, "A review on activities of fifth generation mobile communication system," *Alexandria Engineering Journal*, Vol. 57, No. 2, 1125–1135, June 2018.

7. Chen, Z. and Y. P. Zhang, "FR4 PCB grid array antenna for millimeter-wave 5G mobile communications," *2013 IEEE MTT-S International Microwave Workshop Series on RF and Wireless Technologies for Biomedical and Healthcare Applications (IMWS-BIO)*, 1–3, IEEE, December 2013.

8. Cao, Y., K. S. Chin, W. Che, W. Yang, and E. S. Li, "A compact 38 GHz multibeam antenna array with multifolded butler matrix for 5G applications," *IEEE Antennas and Wireless Propagation Letters*, Vol. 16, 2996–2999, 2017.

9. Agyapong, P. K., M. Iwamura, D. Staehle, W. Kiess, and A. Benjebbour, "Design considerations for a 5G network architecture," *IEEE Communications Magazine*, Vol. 52, No. 11, 65–75, 2014.

10. Fettweis, G. and S. Alamouti, "5G: Personal mobile internet beyond what cellular did to telephony," *IEEE Communications Magazine*, Vol. 52, No. 2, 140–145, 2014.

11. Panwar, N., S. Sharma, and A. K. Singh, "A survey on 5G: The next generation of mobile communication," *Physical Communication*, Vol. 18, 64–84, 2016.

12. Gohil, A., H. Modi, and S. K. Patel, "5G technology of mobile communication: A survey," *2013 International Conference on Intelligent Systems and Signal Processing (ISSP)*, 288–292, IEEE, March 2013.

13. Yu, L. C. and M. R. Kamarudin, "Investigation of patch phase array antenna orientation at 28 GHz for 5G applications," *Procedia Computer Science*, Vol. 86, 47–50, 2016.

14. Ishfaq, M. K., T. A. Rahman, Y. Yamada, and K. Sakakibara, "8×8 phased series fed patch antenna array at 28 GHz for 5G mobile base station antennas," *2017 IEEE-APS Topical Conference on Antennas and Propagation in Wireless Communications (APWC)*, 160–162, IEEE, September 2017.

15. Roy, P., R. K. Vishwakarma, A. Jain, and R. Singh, "Multiband millimeter wave antenna array for 5G communication," *International Conference on Emerging Trends in Electrical Electronics and Sustainable Energy Systems (ICETEESES)*, 102–105, IEEE, March 2016.

16. Ojaroudiparchin, N., M. Shen, and G. F. Pedersen, "Beam-steerable microstrip-fed bow-tie antenna array for fifth generation cellular communications," *2016 10th European Conference on Antennas and Propagation (EuCAP)*, 1–5, IEEE, April 2016.

17. Kumar, A. and P. Kapoor, "Design and performance evaluation of a dual-band antenna for the 5G mobile communication," *IEEE International Conference on Recent Trends in Electronics, Information and Communication Technology (RTEICT)*, 2034–2036, IEEE, May 2016.

18. Thors, B., D. Colombi, Z. Ying, T. Bolin, and C. Törnevik, "Exposure to RF EMF from array antennas in 5G mobile communication equipment," *IEEE Access*, Vol. 4, 7469–7478, 2016.

19. Orakwue, S. I., R. Ngah, and T. A. Rahman, "A two dimensional beam scanning array antenna for 5G wireless communications," *2016 IEEE Wireless Communications and Networking Conference Workshops (WCNCW)*, 433–436, IEEE, April 2016.

20. Wu, X., Y. Zhang, C. X. Wang, G. Goussetis, and M. M. Alwakeel, "28 GHz indoor channel measurements and modelling in laboratory environment using directional antennas," *2015 9th European Conference on Antennas and Propagation (EuCAP)*, 1–5, IEEE, May 2015.

21. Aliakbari, H., A. Abdipour, A. Costanzo, D. Masotti, R. Mirzavand, and P. Mousavi, "ANN-based design of a versatile millimetre-wave slotted patch multi-antenna configuration for 5G scenarios,"

IET Microwaves, Antennas and Propagation, Vol. 11, No. 9, 1288–1295, 2017.

22. Saini, J. and S. K. Agarwal, "Design a single band microstrip patch antenna at 60 GHz millimeter wave for 5G application," *2017 International Conference on Computer, Communications and Electronics (Comptelix)*, 227–230, IEEE, July 2017.

23. Kaur, N. and S. Malhotra, "A review on significance of design parameters of microstrip patch antennas," *2016 5th International Conference on Wireless Networks and Embedded Systems (WECON)*, 1–6, IEEE, October 2016.

24. Goudos, S. K., A. Tsiflikiotis, D. Babas, K. Siakavara, C. Kalialakis, and G. K. Karagiannidis, "Evolutionary design of a dual band E-shaped patch antenna for 5G mobile communications," *2017 6th International Conference on Modern Circuits and Systems Technologies (MOCAST)*, 1–4, IEEE, May 2017.

25. Prasad, P. C. and N. Chattoraj, "Design of compact Ku band microstrip antenna for satellite communication," *2013 International Conference on Communications and Signal Processing (ICCSP)*, 196–200, IEEE, April 2013.

26. Paul, L. C., M. S. Akhter, M. A. Haque, M. R. Islam, M. F. Islam, and M. M. Rahman, "Design and analysis of four elements E, H and combined EH shaped microstrip patch array antenna for wireless applications," *2017 3rd International Conference on Electrical Information and Communication Technology (EICT)*, 1–6, IEEE, December 2017.

27. Chen, Y., R. Jian, and Y. Zhao, "Design of millimeter wave antenna based on fast swarm intelligence algorithm," *Journal of Electronics and Information*, Vol. 1, 2017.

28. Yang, Y. and X. Zhu, "A wideband reconfigurable antenna with 360° beam-steering for 802.11 ac WLAN applications," *IEEE Transactions on Antennas and Propagation*, 2017.

29. Noh, Y., Y. Shin, M. J. Lee, and S. Pyo, "Perpendicularly-fed microstrip antenna with crossed ground slot for GPS application," *2017 14th International Conference on Electrical Engineering/Electronics, Computer, Telecommunications and Information Technology (ECTI-CON)*, 463–464, IEEE, June 2017.

30. Sidhu, E., V. Singh, H. Bhatia, and P. Kuchroo, "Slotted rook shaped novel wide-band microstrip patch antenna for radar altimeter, IMT, WiMAX and C-band satellite downlink applications," *2016 International Conference on Global Trends in Signal Processing, Information Computing and Communication (ICGTSPICC)*, 334–337, IEEE, December 2016.

31. Ali, M. M. and M. T. Islam, "Rectangular with half circle cut-out microstrip patch antenna for C-band applications," *2017 4th International Conference on Advances in Electrical Engineering (ICAEE)*, Dhaka, Bangladesh, 2017.

32. Chauhan, B., S. Vijay, and S. C. Gupta, "Millimeter-wave mobile communications microstrip antenna for 5G-A future antenna," *International Journal of Computer Applications*, Vol. 99, No. 19, 15–18, 2014.

33. Rabbani, M. S. and H. Ghafouri-Shiraz, "Evaluation of gain enhancement in large microstrip antenna arrays for mm-wave applications," *IET Colloquium on Millimetre-Wave and Terahertz Engineering & Technology 2017*, 2017.

34. Ahmad, W. and W. T. Khan, "Small form factor dual band (28/38 GHz) PIFA antenna for 5G applications," *2017 IEEE MTT-S International Conference on Microwaves for Intelligent Mobility (ICMIM)*, 21–24, IEEE, March 2017.

35. Ali, M. M. M. and A. R. Sebak, "Dual band (28/38 GHz) CPW slot directive antenna for future 5G cellular applications," *2016 IEEE International Symposium on Antennas and Propagation (APSURSI)*, 399–400, IEEE, June 2016.

36. Thomas, T., K. Veeraswamy, and G. Charishma, "MM wave MIMO antenna system for UE of 5G mobile communication: Design," *2015 Annual IEEE India Conference (INDICON)*, 1–5, IEEE, December 2015.

37. Sam, C. M. and M. Mokayef, "A wide band slotted microstrip patch antenna for future 5G," *EPH — International Journal of Science And Engineering (ISSN: 2454-2016)*, Vol. 2, No. 7, 19–23, 2016.

38. Rahman, A., M. Y. Ng, A. U. Ahmed, T. Alam, M. J. Singh, and M. T. Islam, "A compact 5G antenna printed on manganese zinc ferrite substrate material," *IEICE Electronics Express*, Vol. 13, No. 11, 20160377–20160377, 2016.

39. Saini, J. and S. K. Agarwal, "T and L slotted patch antenna for future mobile and wireless communication," *2017 8th International Conference on Computing, Communication and Networking Technologies (ICCCNT)*, 1–5, IEEE, July 2017.

40. Singh, M., A. Basu, and S. K. Koul, "Circular patch antenna with quarter wave transformer feed for wireless communication," *2006 Annual IEEE India Conference*, 1–5, IEEE, September 2006.

41. Christ, A., T. Samaras, A. Klingenbock, and N. Kuster, "Characterization of the electromagnetic near-field absorption in layered biological tissue in the frequency range from 30 MHz to 6,000 MHz," *Physics in Medicine and Biology*, Vol. 51, No. 19, 4951–4965, 2006.

42. Hu, Z. H., M. Gallo, Q. Bai, Y. I. Nechayev, P. S. Hall, and M. Bozzettit, "Measurements and simulations for on-body antenna design and propagation studies," *The Second European Conference on Antennas and Propagation, 2007, EuCAP 2007*, 1–7, 2007.

43. Khattak, M. I., R. M. Edwards, M. Shafi, S. Ahmed, R. Shaikh, and F. Khan, "Wet environmental conditions affecting narrow band on-body communication channel for WBANs," *Adhoc and Sensor Wireless Networks*, Vol. 40, Nos. 3–4, 297–312, 16p, 2018.